

X-ray-absorption fine-structure study of the $A15$ superconductors $Nb_3(Sn,Sb)$

J. B. Boyce

Xerox Corporation, Palo Alto Research Center, Palo Alto, California 94304

F. Bridges

Physics Department, University of California-Santa Cruz, Santa Cruz, California 95064

T. Claeson

Physics Department, Chalmers University of Technology, S-412 96 Göteborg, Sweden

T. H. Geballe

Applied Physics Department, Stanford University, Stanford, California 94305

G. W. Hull

Bell Communications Research, Red Bank, New Jersey 07701-7020

N. Kitamura

Aoyama Gakuin University, 6-16-1 Chitosedai, Setagaya-ku, Tokyo 157, Japan

F. Weiss

Laboratoire des Matériaux et du Génie Physique, 38402 Saint-Martin-d'Hères, France

(Received 6 July 1987)

X-ray-absorption fine-structure measurements at the Sn and Sb K edges were made on Nb_3Sn , Nb_3Sb , and $Nb_3Sn_{1-x}Sb_x$ alloys. No temperature-dependent anomalies were noted for the Sn-Nb and Sb-Nb distances or for the broadening in these distances for temperatures from 4.2 K to well above the transition temperatures. The temperature dependence of the broadenings fits an Einstein oscillator model well, with Einstein temperatures of 237 K for Nb_3Sn and 254 K for Nb_3Sb . These results also agree with recent theoretical calculations. The Debye-Waller-type broadening in the Sn-Nb and Sb-Nb distances for the alloys are not equal to one another, but instead are nearly equal to those of the binary end-point compounds, i.e., to Nb_3Sn and Nb_3Sb , respectively.

I. INTRODUCTION

Until the recent discovery of the higher-temperature superconductors based on copper oxides, the highest superconducting transition temperatures, T_c 's, were found in a class of Nb compounds with the $A15$ crystal structure. A wealth of properties of these compounds has been determined over the years, many of which are still not fully understood.¹ The electronic structure displays rich features: a strongly spiked density of states, directional bonds, and anisotropic properties dominated by the chains of near-neighbor A atoms running in the three orthogonal directions in the $A15$ structure of these compounds which have the form A_3B .^{2,3} An anisotropic character is found for the lattice vibrational spectrum^{4,5} and the electron-phonon coupling. Different temperature dependences are found for vibrations on the chains of A atoms and interchain vibrations. Soft phonons develop and a martensitic transformation⁶ to a slightly tetragonally distorted structure occurs for some of the $A15$ compounds as the temperature is lowered. The transformation temperature, T_M , is of the order of a few tens of K, e.g., 37 K for Nb_3Sn . Precursors in the

form of buckled chains are expected well above T_M .

A strongly temperature-dependent electron-phonon coupling has been suggested.⁷ The renormalization of phonons when the interaction with the electron gas becomes the strongest energy in the problem leads to localized ionic vibrations in a two-well potential. The two-well limit with a large electron-phonon coupling goes over to extended phonon states with large zero-point energies and a smaller electron-phonon coupling as the temperature is lowered.

Extended x-ray-absorption fine structure (EXAFS) can be used to measure the local structure: the number and type of neighbors to absorbing atoms, the distances to these neighbors, and the spread in distances. The martensitic transformation, the chain buckling, and the two-well potential in the $A15$ crystals are all expected to give small distortions which may unfortunately be of the same order as the EXAFS experimental resolution of approximately ± 0.01 Å. However, the temperature dependence of the Debye-Waller-type broadening of the near-neighbor peaks in the pair distribution function also yields information about the vibrational states. Note that the square of the width measured in EXAFS, σ^2 , is

not the deviation from the lattice position as for the conventional Debye-Waller factor, but rather a spread in the interatomic distances. Hence correlation effects are of importance. These have been taken into account by Weber⁵ in a calculation of σ^2 versus temperature for Nb_3Sn and Nb_3Sb .

This study compares the EXAFS of Nb_3Sn , Nb_3Sb , and alloys of these compounds. Nb_3Sn is a high- T_c superconductor (≈ 18 K) with a large electron-phonon coupling strength ($\lambda \approx 1.4$). It displays a martensitic transformation at 37 K (Ref. 8) and has highly anisotropic electron and phonon behavior with different temperature dependences for different bonds and phonon modes. For x-ray experiments, Nb_3Sb is almost the same as Nb_3Sn since Sn and Sb are neighbors in the periodic table. Otherwise, it is significantly different: a low T_c (≈ 0.4 K), a small λ (≈ 0.4), no substantial softening of the lattice at low T , no martensitic transformation, and more isotropic. Nb_3Sn and Nb_3Sb form a solid solution with the A15 structure. There is a change of the c/a ratio in the distorted state from $c/a < 1$ at Nb_3Sn to $c/a > 1$ as the Sb concentration exceeds about 10%. Actually, it is possible to obtain both deformations⁸ within a certain concentration interval: first $c/a < 1$ and then $c/a > 1$ as the temperature is lowered further. The $\text{Nb}_3\text{Sn}_{1-x}\text{Sb}_x$ alloy has been reported to separate into two A15 phases in an intermediate composition range, one Nb_3Sn rich and one Nb_3Sb rich.⁹

We have measured the EXAFS at the Sn and Sb K edges in $\text{Nb}_3\text{Sn}_{1-x}\text{Sb}_x$ alloys and the binary endpoint compounds. Less anomalous (and interesting) properties are expected around the Sn and Sb atoms than around the Nb atoms. However, the structural information in the vicinity of the Sn and Sb atoms is more easily interpreted for the A15 structure since the first neighbor Nb shell around the Sn or Sb atoms is well separated from the second and following neighbor shells. This is in contrast to the situation around the Nb atoms, where the EXAFS peaks due to the first, second, and third shells interfere and so are not as easily separable. This study concentrates on the temperature dependence of σ^2 for the nearest-neighbor distances.

II. EXPERIMENTS

Nb_3Sn and $\text{Nb}_3(\text{Sn,Sb})$ samples were grown from the melt as described in Ref. 8. Such samples had previously been used to map out the tetragonal phase transformations in $\text{Nb}_3\text{Sn}_{1-x}\text{Sb}_x$. We used samples with $x = 0.0, 0.075, 0.11, 0.22, 0.25, 0.37, 0.63,$ and 1.0 . Two Nb_3Sb samples were investigated: one made at Bell Labs and one grown from the gas phase at Grenoble. A sample of $\text{Nb}_3\text{Sn}_{1-x}\text{Sb}_x$, with $x \approx 0.5$, was also grown using the Bell Labs technique.

The crystals were ground into a fine powder, mixed with epoxy, and molded into strips with a thickness of about 2.5 absorption lengths at the Sn and Sb K edges. The x-ray absorption spectra of the samples were measured at several temperatures between 4.2 and 300 K. In addition, for the two binary compounds, measurements were made above room temperature, up to about 350°C.

Data were taken on the wiggler beamline IV-1 of the Stanford Synchrotron Radiation Laboratory, using a Si(220) monochromator. The double-crystal monochromator was detuned on the rocking curve to roughly $\frac{1}{2}$ maximum intensity to minimize harmonic reflections. Ionization counters with Ne and Ar gas were used to measure the incident and transmitted x-ray intensities, respectively.

III. RESULTS

The EXAFS data were reduced in the usual way.¹⁰ The EXAFS k -space spectrum on the Sn and Sb K edges was Fourier transformed to real space using a k window of $3.8\text{--}15.8 \text{ \AA}^{-1}$ broadened by a Gaussian of width 0.5 \AA^{-1} . An example of the EXAFS data in k space at the Sn K edge for $\text{Nb}_3\text{Sn}_{0.75}\text{Sb}_{0.25}$ is shown in Fig. 1(a). The Sb K edge intrudes on this spectrum at $k = 18.4 \text{ \AA}^{-1}$. The Fourier transform to real space is shown in Fig. 1(b). The peaks give the nearest-neighbor locations but are shifted inward by a small amount as a result of a phase shift in the scattering process. The first neighbor distances from the absorbing atom (Sn or Sb) to the Nb is easily determined relative to that distance in the

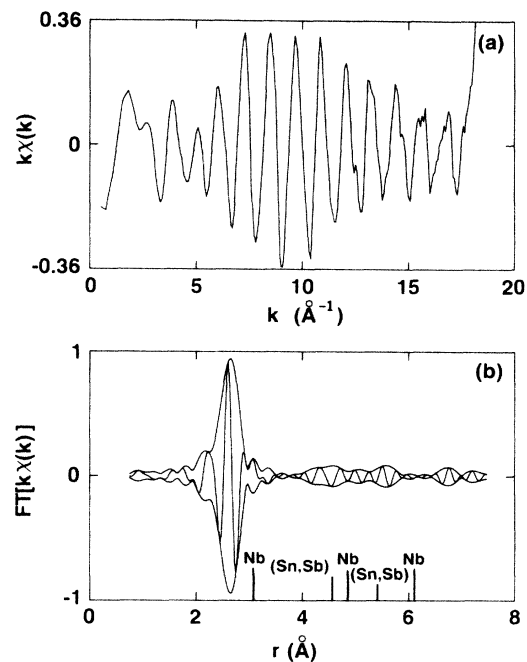


FIG. 1. (a) EXAFS in k space above the Sn K edge for $\text{Nb}_3\text{Sn}_{0.75}\text{Sb}_{0.25}$ at 4.2 K. The sharp rise above 18 \AA^{-1} is due to the Sb K edge which is 1290 eV above that of Sn, i.e., at 18.4 \AA^{-1} . (b) The magnitude (envelope) and the real part of the Fourier transform of the EXAFS, $k\chi(k)$ of part (a), over a k -space window of $3.8\text{--}15.8 \text{ \AA}^{-1}$ broadened by a Gaussian of width 0.5 \AA^{-1} . The vertical lines show the locations of the first five shells of neighbors around the absorbing Sn atoms, with the height being proportional to the number of neighbors (12 Nb first neighbors, 8 Sn and Sb second neighbors, . . .). Phase shifts have to be added to the EXAFS peak positions to give the corresponding distances in the pair distribution function.

structural standard, i.e., Nb_3Sn or Nb_3Sb . In the alloys, as well as in the binary compounds, the further neighbors are not as well distinguished due to greater thermal disorder in addition to possible structural disorder.

The EXAFS in r space at the Sn K edge for Nb_3Sn is shown for a few temperatures in Fig. 2. Due to an increase of σ^2 with temperature, the structure is broadened significantly. This causes an increase in the peak width with a subsequent reduction in peak height. Note, however, that no substantial changes in near-neighbor distances with temperature are evident.

For a quantitative comparison, data in real space were fit to structural standards in order to determine any change in neighbor distances and spreads in distance with temperature. The real-space EXAFS signature of either the same sample or the $\text{Nb}_3\text{Sn}_{1-x}\text{Sb}_x$ sample with $x \approx 0.5$, both at 4.2 K, were used for the comparisons. Surprisingly, the latter gave the sharpest signature, i.e., the smallest spread of nearest-neighbor distances. The comparison range in these r space fits at different temperatures was 2.3–2.9 Å for both the Sn and Sb edge data.

In these fits, no significant changes in the nearest-neighbor distances and coordination numbers were noted over the entire temperature range. Any distortion or change must, therefore, be smaller than the experimental resolution of about ± 0.01 Å in distance and ± 1 neighbor in coordination (out of 12 Nb first neighbors). The only substantial change with temperature in the near-neighbor environment is an increase in the width of the pair distribution function, the Debye-Waller-type

broadening. Since the same sample at 4.2 K is used as the structural standard, the quantity determined is the change in width, namely,

$$\Delta\sigma^2(T) = \sigma^2(T) - \sigma^2(4.2 \text{ K, same sample}). \quad (1)$$

$\Delta\sigma^2$ is given as a function of temperature in Fig. 3 for the Sn-Nb and the Sb-Nb distances in Nb_3Sn and Nb_3Sb . The solid lines are the theoretical predictions of an Einstein-oscillator model with the Einstein frequency adjusted to fit the data (see discussion below). Figure 4 compares these data with the theoretical predictions of Weber,⁵ with no adjustments other than the subtraction of a constant, the zero-point motion, to yield $\Delta\sigma^2$. The linear slope of $\Delta\sigma^2$ versus T , for high T , is larger for Nb_3Sn than it is for Nb_3Sb but not quite as large a difference as predicted by Weber.⁵ On the whole, the agreement between theory and experiment is very good. Figure 5 compares the $\Delta\sigma^2(T)$ for the alloys with the results for Nb_3Sn and Nb_3Sb . It appears that $\Delta\sigma^2$ for the Sn-Nb distance has the same temperature dependence in the $\text{Nb}_3(\text{Sn,Sb})$ alloys as in Nb_3Sn itself. Likewise, there is a similar tendency for the $\Delta\sigma^2$ of the Sb-Nb distance to correlate with that for pure Nb_3Sb rather than the one for the Sn-Nb distance in the same sample. The possible observation of very local correlations in the alloys is interesting, but the measurements should be extended to higher temperatures in order to fully establish such behavior. A similar analysis for the further neighbor peaks was not carried out since these peaks are significantly smaller (see Fig. 2).

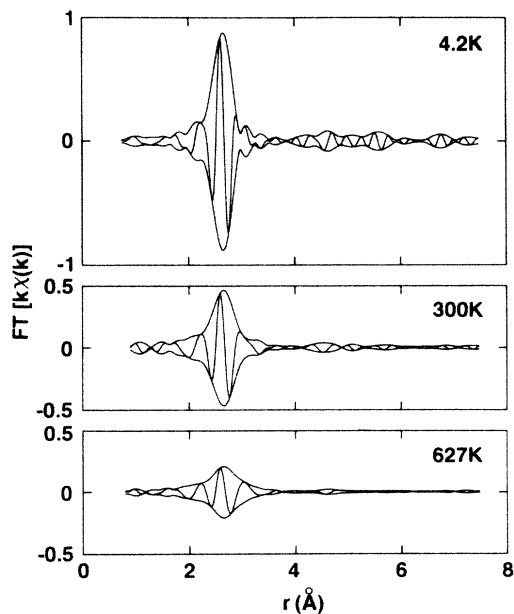


FIG. 2. The EXAFS in r space for Nb_3Sn at 4.2, 300, and 627 K. The data were Fourier transformed from k space using a window of 3.8 – 15.8 Å⁻¹, Gaussian broadened by 0.5 Å⁻¹. The large changes in the peaks with increasing temperature are due to the increase in the thermal width of the pair distribution functions.

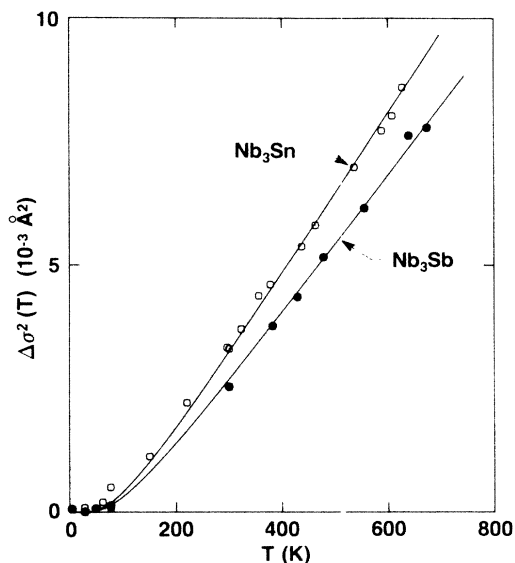


FIG. 3. The Debye-Waller-type broadening, $\Delta\sigma^2(T) = \sigma^2(T) - \sigma^2(4.2 \text{ K, same sample})$, of the nearest-neighbor distances in Nb_3Sn (open circles) and Nb_3Sb (solid circles) from the EXAFS at the Sn and Sb K edges, respectively. The uncertainties in the data are approximately $\pm 0.2 \times 10^{-3}$ Å². The solid lines are fits to the data using an Einstein-oscillator model, Eq. (2), with the adjusted parameter being the Einstein temperature, yielding $\theta_E(\text{Nb}_3\text{Sn}) = 237$ K and $\theta_E(\text{Nb}_3\text{Sb}) = 254$ K.

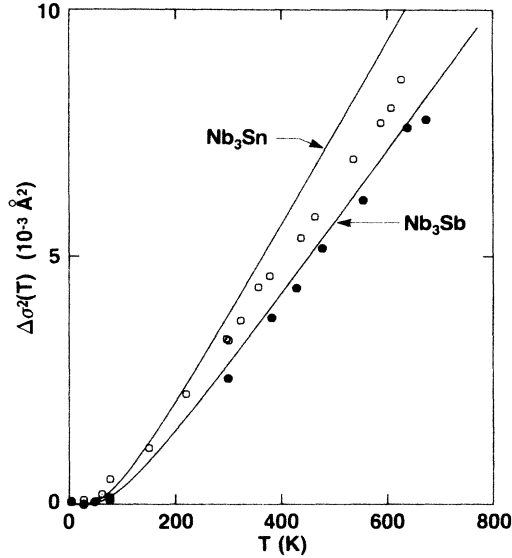


FIG. 4. The Debye-Waller-type broadening, $\Delta\sigma^2(T) = \sigma^2(T) - \sigma^2(4.2 \text{ K})$, of the nearest-neighbor distances in Nb_3Sn (open circles) and Nb_3Sb (solid circles) from the EXAFS at the Sn and Sb *K* edges, respectively. The uncertainties in the data are approximately $\pm 0.2 \times 10^{-3} \text{ \AA}^2$. The solid lines are from theoretical calculations (Ref. 5) of Weber with no adjustments. These curves are very similar to those for an Einstein oscillator with Einstein temperatures of $\theta_E^{\text{theory}}(\text{Nb}_3\text{Sn}) = 221 \text{ K}$ and $\theta_E^{\text{theory}}(\text{Nb}_3\text{Sb}) = 249 \text{ K}$.

Plots similar to Figs. 3–5 are obtained when comparing the samples at different temperatures to the $\approx 50:50$ $\text{Nb}_3(\text{Sn,Sb})$ sample at 4.2 K. However, in such plots, the background in the form of $\sigma^2(4.2 \text{ K})$ is smaller for the 50:50 alloy. The Nb_3Sn samples have a larger $\Delta\sigma^2$ value than Nb_3Sb . The $x = 0.37$ and 0.63 samples showed smaller EXAFS amplitudes, but the values for $\Delta\sigma^2(T)$ agree with the results from the other alloys. The smaller amplitudes are most probably caused by the interference between two *A15* phases with slightly different lattice constants.^{8,9} X-ray diffraction showed extra peaks, and the superconducting transition regions were broad for these two samples.

IV. DISCUSSION

For the temperature variation of the observed Debye-Waller-like broadening of the pair distribution function with the assumption that the individual bonds can be treated as Einstein oscillators, we have^{11,12,13}

$$\sigma^2(T) \approx [\hbar / (2\mu\omega_E)] \coth(\hbar\omega_E / 2k_B T), \quad (2)$$

where μ is the reduced mass of the pair of atoms and ω_E is the Einstein frequency, which can be considered as a measure of the average phonon frequency for the actual phonon density of states. At high temperatures, $\sigma^2(T) \approx k_B T / \mu\omega_E^2$. As discussed above, the absolute width σ^2 was not determined but rather $\Delta\sigma^2(T)$, given by Eq. (1). Equation (2) fits the data well, as shown in

Fig. 3, yielding the following Einstein temperatures, $\theta_E = \hbar\omega_E / k_B$:

$$\theta_E(\text{Nb}_3\text{Sn}) = 237 \text{ K}$$

and

$$\theta_E(\text{Nb}_3\text{Sb}) = 254 \text{ K}.$$

The value of θ_E (or ω_E) for Nb_3Sn is 7% smaller than for Nb_3Sb .

Our results on Nb_3Sn differ from those of Heald and Tranquada¹⁴ (HT) in that their data over the smaller temperature range of 4.2 to 300 K do not fit a single Einstein-oscillator model. The two sets of data agree well at 300 K and below 100 K, but HT observe a smaller $\Delta\sigma^2(T)$ than ours for the three data points in the temperature interval of 100 to 250 K. This difference causes a deviation from a single Einstein-oscillator result which they interpret as a softening of the Sn-Nb vibrations as the temperature is lowered toward $T_M \approx 37 \text{ K}$. Our data show no such softening but rather agree well with an Einstein-oscillator model and the theoretical calculations of Weber,⁵ discussed below. The reasons for this discrepancy are unknown but may lie in possible differences in the samples; HT point out that large static disorder could also explain their results. In addition, it should be noted that the actual differences between the two sets of data do not substantially exceed the error

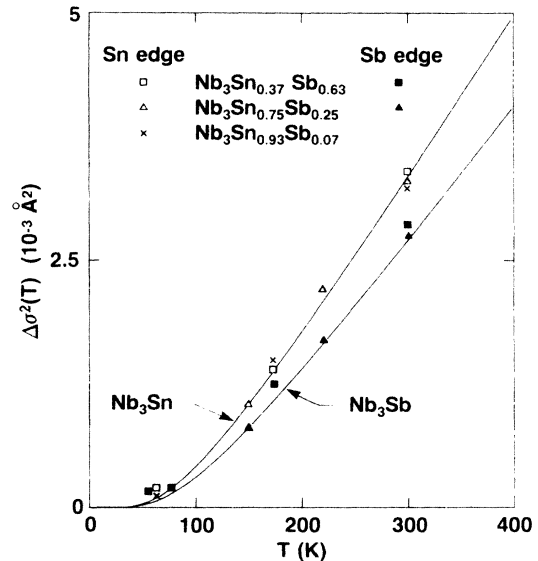


FIG. 5. The Debye-Waller-type broadening of the nearest-neighbor distances in $\text{Nb}_3(\text{Sn,Sb})$ alloys at the Sn *K* edge (open symbols) and Sb *K* edge (solid symbols). The uncertainties in the data are approximately $\pm 0.2 \times 10^{-3} \text{ \AA}^2$. The solid lines are the Einstein oscillator model fits to the data on the pure binary compounds, Nb_3Sn and Nb_3Sb , shown in Fig. 3. Note that the individual widths in the alloys differ from one another but are approximately equal to the widths in the respective binary compounds, i.e., the Sn-Nb width in the alloys is about the same as that in the pure Nb_3Sn compound, with a similar situation for the Sb-Nb width.

bars, e.g., HT find $\Delta\sigma^2(242\text{ K}) \approx (1.75 \pm 0.2) \times 10^{-3} \text{ \AA}^2$ compared with our $\Delta\sigma^2(220\text{ K}) = (2.22 \pm 0.2) \times 10^{-3} \text{ \AA}^2$.

Recently, Weber⁵ has calculated $\sigma^2(T)$ for the interatomic distances in Nb_3Sn and Nb_3Sb , i.e., the σ^2 that is observed in the EXAFS. Figure 4 shows that these calculations are in reasonably good agreement with the experimental results. Weber used highly accurate lattice dynamical models for the phonon-dispersion curves and included the correlation of the pair of atoms in the A_3B structure that results because of the strong radial spring constants between the A - B pairs. These phonon curves are consistent with neutron scattering measurements in which it is found that the vibrational modes in Nb_3Sn are about 10% softer than in Nb_3Sb . (Some intra-Nb chain modes are lowered much more than 10% and are the modes which are supposed to couple strongly to the electrons and cause the high T_c .) This 10% difference agrees well with our 7% difference. Weber's calculated values of $\sigma^2(T)$ can be fit extremely well to a simple Einstein model, with the resulting Einstein temperatures of

$$\theta_E^{\text{theory}}(\text{Nb}_3\text{Sn}) = 221\text{ K}$$

and

$$\theta_E^{\text{theory}}(\text{Nb}_3\text{Sb}) = 249\text{ K}.$$

These values predict a 13% softer value for Nb_3Sn compared with our measured 7% difference. The theoretical and experimental values agree more closely for Nb_3Sb than for Nb_3Sn , as is evident in Fig. 4.

Nb_3Sn is expected to be similar to V_3Si in which there is a pileup of charge, forming a quasibond, between Si and V at room temperature but not at low temperatures.³ A similar charge concentration might explain the apparent Sn-Nb correlation that remains in the ternary alloys, leading to different $\Delta\sigma$'s for Sn-Nb and Sb-Nb in the same alloy. This is indicated, although weakly, in the alloy data at 300 K, Fig. 5, where it is seen that the individual widths differ from one another but are approximately equal to the corresponding widths in the pure binary compounds. A somewhat related situation has been observed in semiconductor pseudobinary alloys.¹⁵ For these $(A_xB_{(1-x)})C$ alloys it is noted that the A - C and B - C distances are different from one another and remain roughly constant as the concentration is varied. This is the case even though the average lattice constant varies linearly with x , i.e., follows Vegard's law.

Yu and Anderson⁷ have proposed an interesting model for $A15$ superconductors in order to explain several anomalous electron-phonon properties, e.g., the saturation of the electrical resistivity, ρ , at high temperature and the large discrepancy between the high-temperature λ value derived from the resistivity and the low-temperature λ from superconductivity. They suggest that the electron-phonon coupling can, in the limit of very strong coupling, lead to a two-well ionic potential at high temperature. Localized vibrations are due to ions vibrating in either of them and hopping between the

two positions. The electron scattering is high. At lower temperature, the oscillators become less anharmonic, the neglected interoscillator coupling reasserts itself, and extended harmonic phonons can be defined. A study of localized phonons in the Mo-Re system by superconducting tunneling has recently given support¹⁶ to this Yu-Anderson model.

The high-temperature separation of the two wells would be too small to distinguish (being also thermally blurred) in an EXAFS experiment. However, an anomalous Debye-Waller factor⁷ might be remnant at low temperature. In our case, one might expect differences in the σ^2 's themselves and in their temperature dependences for Nb_3Sn and Nb_3Sb . The temperature dependences of the resistivities of the two compounds are similar but the saturation (and renormalization) occurs at different temperatures. Furthermore, the electron-phonon coupling, λ , is much larger for Nb_3Sn . Hence one would expect the renormalization to occur at a lower temperature in Nb_3Sn than in Nb_3Sb .

No obvious anomalies in $\Delta\sigma^2(T)$ were evident in either Nb_3Sn or Nb_3Sb (see Figs. 3 and 4). Their temperature variations were qualitatively the same with a linear relationship over the interesting temperature interval. The larger $\Delta\sigma^2$ value for Nb_3Sn is expected from Weber's model,⁵ but the measured difference is small. The possible localized character of the relative displacements in the ternary alloys could also favor the Yu-Anderson model, but again it is questionable at this stage since a similar situation is observed in other alloys.

In conclusion, Nb_3Sn and Nb_3Sb show a similar temperature dependence for the Debye-Waller-type broadening of the Sn-Nb and Sb-Nb near-neighbor distances. No anomalies are observed in the temperature range of 4.2 to 627 K. Good agreement between theory and experiment is found, and both agree well with a simple Einstein-oscillator model. The experimental Einstein temperatures are $\theta_E(\text{Nb}_3\text{Sn}) = 237\text{ K}$ and $\theta_E(\text{Nb}_3\text{Sb}) = 254\text{ K}$. The small difference can be explained by the different phonon spectra. A localized vibration behavior in the ternary alloys is indicated, but additional measurements are needed to further quantify this conclusion.

ACKNOWLEDGMENTS

Assistance in the sample preparation by Y. Inada and R. Madar, in an x-ray diffraction recording by R. Howland and in the data collection by G. Dimino is acknowledged. The experiments were performed at Stanford Synchrotron Radiation Laboratory, which is supported by the U.S. Department of Energy (Basic Energy Sciences Program) and the National Institutes of Health (Biotechnology Division). Financial support was given by the Swedish Natural Science Research Council, and by National Science Foundation (NFS) Grant No. DMR-85-05549. One of us (T.C.) wants to thank Xerox Corporation and Stanford University for their hospitality.

- ¹For a review see, e.g., L. R. Testardi, *Rev. Mod. Phys.* **47**, 637 (1975); J. Muller, *Rep. Prog. Phys.* **43**, 641 (1980).
- ²B. M. Klein, L. L. Boyer, D. A. Papaconstantopoulos, and L. F. Mattheiss, *Phys. Rev. B* **18**, 6411 (1978).
- ³J. L. Staudenmann, B. DeFacio, and C. Stassis, *Phys. Rev.* **27**, 4186 (1983).
- ⁴G. S. Cargill, III, R. F. Boehme, and W. Weber, *Phys. Rev. Lett.* **50**, 1391 (1983).
- ⁵W. Weber, *J. Phys. F* **17**, 27 (1987).
- ⁶See, e.g., R. N. Bhatt and W. L. McMillan, *Phys. Rev. B* **14**, 1007 (1976).
- ⁷C. C. Yu and P. W. Anderson, *Phys. Rev.* **29**, 6165 (1984).
- ⁸Y. Fujii, J. B. Hastings, M. Kaplan, G. Shirane, Y. Inada, and N. Kitamura, *Phys. Rev. B* **25**, 364 (1982).
- ⁹F. J. Bachner, J. B. Goodenough, and H. C. Gatos, *J. Phys. Chem. Solids* **28**, 889 (1967).
- ¹⁰T. M. Hayes and J. B. Boyce, in *Solid State Physics*, edited by H. Ehrenreich, F. Seitz, and D. Turnbull (Academic, New York, 1982), Vol. 37, pp. 173–351.
- ¹¹E. Sevillano, H. Meuth, and J. J. Rehr, *Phys. Rev. B* **20**, 4908 (1979).
- ¹²T. Claeson, J. B. Boyce, and T. M. Geballe, *Phys. Rev. B* **25**, 6666 (1982).
- ¹³G. S. Knapp, H. K. Pan, and J. M. Tranquada, *Phys. Rev. B* **32**, 2006 (1985).
- ¹⁴S. M. Heald and J. M. Tranquada, *Adv. Cryog. Eng.* **32**, 471 (1985).
- ¹⁵J. B. Boyce and J. C. Mikkelsen, Jr., in *Ternary and Multinary Compounds*, edited by S. K. Deb and Alex Zunger (Materials Research Society, Pittsburgh, 1987), p. 359.
- ¹⁶D. P. Shum, A. Bevolo, J. L. Staudenmann, and E. L. Wolf, *Phys. Rev. Lett.* **57**, 2987 (1986).